Title:	Punching resistance and flexural behaviour of continuous flat slabs
Authors:	Einpaul J., Fernández Ruiz M., Muttoni A.
Published in:	Proc. of the 10th fib International PhD Symposium in Civil Engineering, Quebec
Pages:	pp. 425-436
Country:	Canada
Year of publication:	2014
Type of publication:	Peer reviewed conference paper

Please quote as:	Einpaul J., Fernández Ruiz M., Muttoni A., *Punching resistance and flexural behaviour of continuous flat slabs*, Proc. of the 10th fib International PhD Symposium in Civil Engineering, Quebec, Canada, 2014, pp. 425-436.

Punching resistance and flexural behaviour of continuous flat slabs

Jürgen Einpaul, Miguel Fernández Ruiz, Aurelio Muttoni

School of Architecture, Civil and Environmental Engineering,
École Polytechnique Fédérale de Lausanne,
Station 18, CH-1015 Lausanne, Switzerland

Abstract

The punching resistance of actual reinforced concrete flat slabs is potentially influenced by the compressive membrane action, which may significantly increase their resistance compared to isolated laboratory specimens. However, design codes have been developed using the results of laboratory experiments and therefore usually neglect this phenomenon.

In this paper, a numerical model is presented to describe the behaviour of continuous and confined flat slabs under distributed loads. The flexural strength and stiffness are shown to increase due to the redistribution of moments and in-plane forces in the slab arising from the confinement of the slab dilation. The failure criterion of the Critical Shear Crack Theory is applied to predict the punching strength. The modelling results are compared to experimental data of some unconventional punching tests from the literature and satisfactory correlation is found.

1 Introduction

Punching shear is often the governing mode of failure in slender flat slabs. The code provisions for this verification are developed using results of laboratory tests performed on isolated specimens of limited size. Typically, the test setup is designed in a manner that avoids the development of in-plane forces in the specimen.

The punching resistances of actual flat slabs have been observed to potentially exceed the values obtained by laboratory testing [1]. This has been attributed to the development of compressive membrane action in the slab due to its confinement [2]. Models based on the theory of plasticity have been used to take this effect into account [3, 4]. According to a rigid-plastic solution [4], the load-carrying capacity of the element obtains a maximum value at zero deflection ($w = 0$) ((1) in Fig. 1) and diminishes with increasing w due to the decreasing rise of the compression arch (2). At deflections close to the thickness of the element h, the capacity tends to the unconfined yield-line solution q_{yl} (3). For predicting the increasing branch of the load-deflection curve, elastic-plastic modes [5] have to be used. These models consider that the supports have a certain lateral restraining stiffness that does not allow the development of full confining force at zero deflection ((4) in Fig. 1). However, determining an appropriate stiffness remains a problem that has not been satisfactorily solved [6].

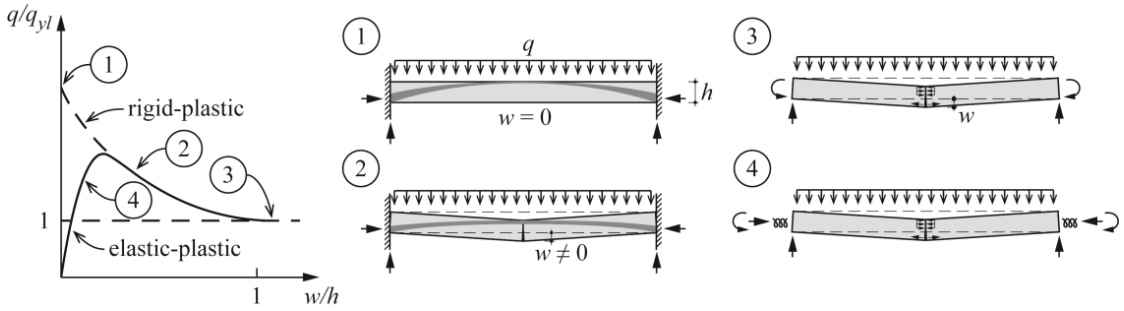

Fig. 1 Membrane effect in confined reinforced concrete elements according to rigid-plastic and elastic-plastic approaches

Unlike actual continuous slabs, the test specimens typically model only the hogging moment area around the support. This approach simplifies the testing, as no bending moment has to be applied at the edge of the specimen to model the influence of the surrounding slab. The extent of the hogging moment area is usually determined by an elastic analysis of the slab, which for regular span bays leads to a distance of approximately 0.22 L from the centre of the column to the line of moment con-

traflexure. This method does not take into account the influence of moment redistribution between hogging and sagging moments that can occur in continuous slabs due to their non-linear behaviour (cracking of concrete and yielding of reinforcement). The applicability of the calculation models therefore depends on the correctness of the assumption of elastic moment distribution.

2 Numerical model

In the current research, a numerical model based on the work done previously at École Polytechnique Fédérale de Lausanne [7, 8] is developed to determine the deformations and internal forces of a two-way slab submitted to a concentrated support reaction.

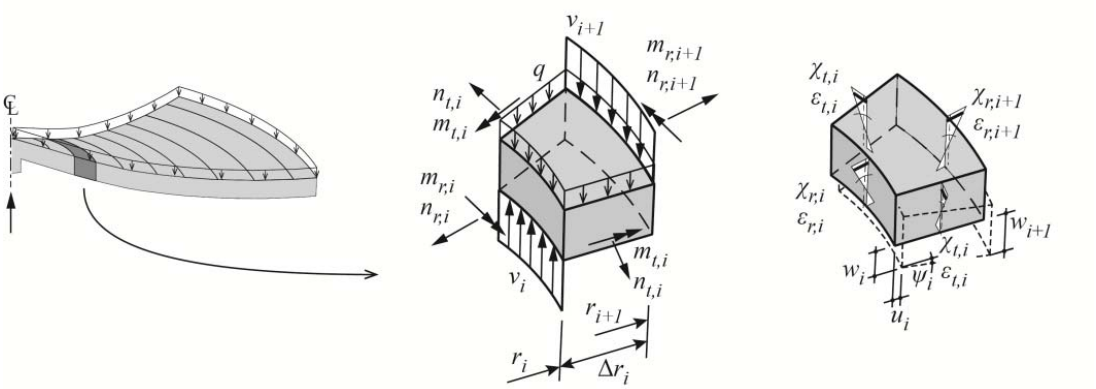

Fig. 2 Axisymmetric sector element: forces acting on the element, deformations and displacements of the element

The slab is divided into axisymmetric elements (Fig. 2). For each element, equations for the equilibrium of internal forces (Eq. 1) and the compatibility of deformations (Eq. 2) can be written:

$$m_{r,i+1} \cdot r_{i+1} - m_{r,i} \cdot r_i - m_{t,i} \cdot \Delta r_i + v_{i+1} \cdot \Delta r_i \cdot r_{i+1} + q_i A_i \left(r_q - r_i \right) = 0 \tag{1a}$$

$$n_{r,i+1} \cdot r_{i+1} - n_{r,i} \cdot r_i - n_{t,i} \cdot \Delta r_i = 0 \tag{1b}$$

$$\chi_{t,i} = \frac{-\psi_i + \chi_{r,i} \cdot \Delta r_i / 2}{r_i + \Delta r_i / 2} \tag{2a}$$

$$\varepsilon_{t,i} = \frac{u_i + \varepsilon_{r,i} \cdot \Delta r_i / 2}{r_i + \Delta r_i / 2} \tag{2b}$$

A layered non-linear sectional analysis can provide the moment-curvature relationship to relate the internal forces to the deformations. In the current research, a simplified multi-linear relationship between bending moment (m) along with normal force (n) and curvature (χ) along with expansion (ε) is utilized in order to facilitate calculations:

$$\left(m_i , n_i \right) = f_{multi-lin} \left(\chi_i , \varepsilon_i \right) \tag{3}$$

The calculation is started at the first element in the centre of the slab ($r_i = 0$), where rotation ψ, radial displacement u and deflection w are equal to zero. A state of deformations ($\chi_{r,1}$, $\varepsilon_{r,1}$) is assumed at the internal radial edge of the first element. Tangential forces acting on the element are found by using the geometrical compatibility equations (2) and the multi-linear sectional response (3). Using the force equilibrium equations (1), the internal forces at the other radial edge of the element (at r_{i+1}) are determined. Then, the state of deformations ($\chi_{r,i+1}$, $\varepsilon_{r,i+1}$) at r_{i+1} is found from the inverse of Eq. 3, after which the rotation ψ_{i+1}, the radial displacement u_{i+1} and the deflection w_{i+1} are determined. Thereafter, the calculation can be repeated for the next element. At the outer edge of the slab, two boundary conditions result from the assumed state of deformations at the centre of the slab:

$$\left(c_{I,\,edge} , c_{II,\,edge} \right) = f \left(\chi_{r,1} , \varepsilon_{r,1} \right) \tag{4}$$

The state of deformations at the first element leading to the desired boundary conditions is found iteratively. The boundary conditions can model different boundary conditions of a slab, for example:

- ($m_{r,edge}$ = 0, $n_{r,edge}$ = 0) for the edge of an isolated test specimen;
- (ψ_{edge} = 0, u_{edge} = 0) for the mid-span of a continuous slab with perfect external confinement;
- (ψ_{edge} = 0, $n_{r,edge}$ = 0) for the mid-span of a continuous slab with no external confinement.

3 Results of the modelling

As an example, the model is applied to predict the deformations of a typical slab in a building with a span of L = 7 m between the axes of the columns, thickness h = 250 mm, effective depth d = 210 mm, concrete strength f_c = 35 N/mm^2, flexural reinforcement ratio ρ_1 = 1.0 % above the columns and ρ_2 = 0.5 % at mid-span with the yield strength of reinforcing steel f_y = 550 N/mm^2. The diameter of the columns is c = 260 mm. The load is applied uniformly over the whole slab.

The slab is modelled firstly as an isolated hogging moment area (with a radius of 0.22·L), secondly as a continuous slab (radius 0.7·L that leads to a size of the hogging moment area of 0.22·L in the uncracked phase) but neglecting the presence of in-plane forces (equilibrium conditions (1b) and (2b)), thirdly as a continuous slab taking into account the in-plane forces but applying no external confinement (a self-confined slab) and lastly as a continuous slab with perfectly restrained horizontal displacement.

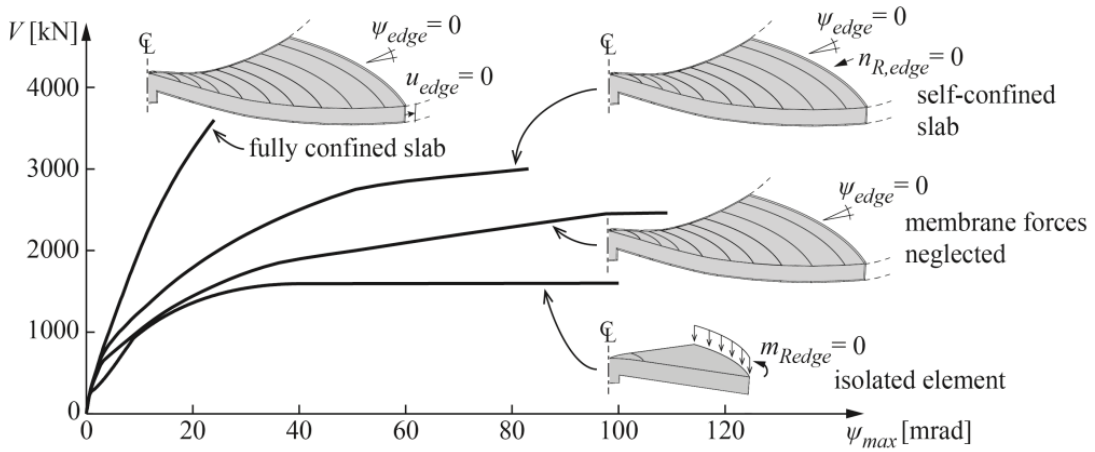

Fig. 3 Example of the application of the model using different edge conditions

Fig. 3 presents the relationship between the shear force and the slab rotation at the line of moment contraflexure. In accordance with the models based on the theory of plasticity, taking into account the in-plane forces significantly increases the flexural strength and stiffness of the slab. It is interesting to note that even only the stiffness of the slab portion outside the hogging moment area provides a considerable amount of confinement and significantly decreases the deflections.

3.1 Effect of moment redistribution

As seen in Fig. 3 on the load-rotation curve of the continuous slab with membrane forces neglected, an important part of the increase of strength and stiffness results from taking into account the activation of sagging moment in mid-span.

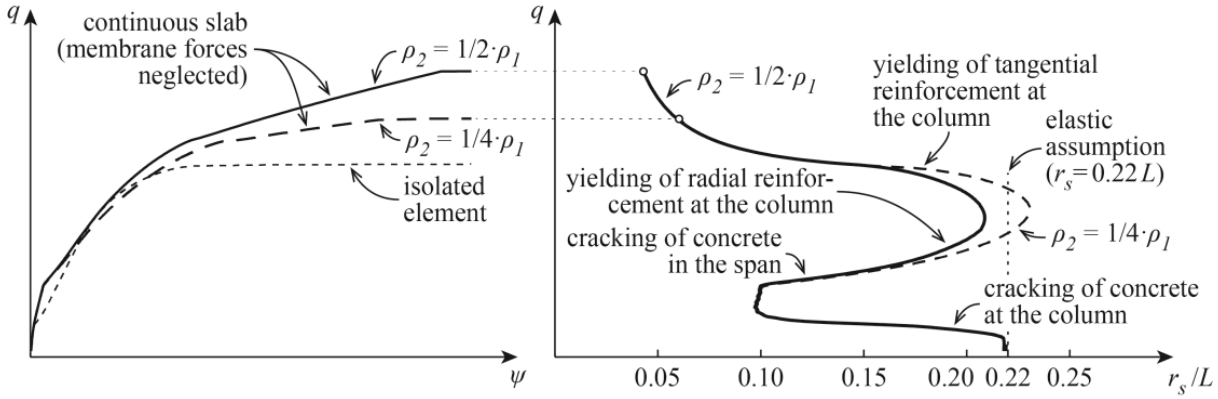

Fig. 4 Load-rotation curves of an isolated specimen and continuous slabs with different span reinforcement ratios (left); distance to the line of moment contraflexure (right)

Fig. 4 (right) shows the distance to the line of moment contraflexure depending on the load. In Fig. 4 (left), the load-rotation curve of an isolated element is compared to the curve for continuous slabs with different amounts of mid-span reinforcement. It can be seen that while the initial load-rotation responses of the continuous slab and a corresponding isolated element are similar, the difference increases at higher levels of load and rotation. This is explained by the changes of the location of the line of moment contraflexure in the continuous model. As the cracking of concrete and yielding of reinforcing bars at the column and in mid-span occur at different loads levels, moments are redistributed between hogging and sagging moments. The distance to the line of moment contraflexure approaches the elastic estimate of 0.22 L only after the concrete is cracked both in the span and at the column but reinforcement does has not yet reached yielding in the tangential direction at the column.

4 Failure criterion of the critical shear crack theory

A brittle punching failure often occurs before the full development of flexural deformations described above. The mechanical model of the Critical Shear Crack Theory [9] predicts that the failure occurs where the load-rotation curve intersects with the failure criterion. The failure criterion depends on the opening (proportional to $\psi \cdot d$) and the roughness (proportional to the maximum aggregate size d_g; d_{g0} = 16 mm) of the inclined critical crack around the face of the column [9]:

$$V_R = \frac{3/4 \cdot b_0 d \sqrt{f_c}}{1 + 15 \dfrac{\psi \cdot d}{d_{g0} + d_g}} \tag{5}$$

where b_0 indicates the length of the control perimeter that is located at d/2 from the edge of the column. The failure criterion is therefore shifted upwards with increasing column size. For shear-reinforced slabs, it has been shown [10] that the failure criterion for slabs with sufficient amounts of shear reinforcement is a multiple of the failure criterion for slabs without shear reinforcement (5).

The compressive in-plane force in the vicinity of the column may have an influence on the failure criterion by decreasing the opening of the critical crack. For prestressed slabs, good results were obtained by reducing the product $\psi \cdot d$ in equation (5) [11]. However, this influence is not taken into account in the current paper.

Fig. 5 shows the application of CSCT for the example slab presented in Fig. 3. For slabs with small column sizes or without shear reinforcement, the increase in the predicted punching resistance is less significant. However, the increase is more important for slabs with large amounts of highly efficient shear reinforcement (like double-headed shear studs) or for slabs on larger columns. This suggests that for slabs with shear reinforcement, testing punching on isolated specimens might not be representative of actual slabs because of the significantly lower flexural strength of the isolated specimens compared to continuous slabs.

It should also be noted that while the punching strength increases due to the confinement, the deformation capacity of the slab decreases. This could lead to higher than predicted forces generated by imposed displacements.

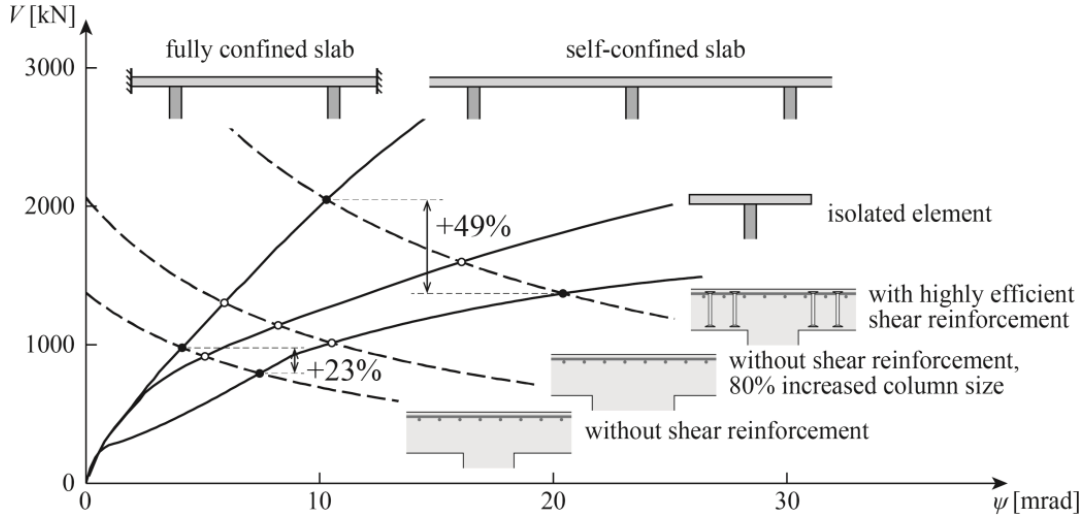

Fig. 5 Load-rotation curve and failure criteria for isolated and continuous slabs

5 Comparison with test results

The predictions of the numerical model together with the failure criterion of CSCT were compared to the results of some unconventional punching tests reported in the literature:

- A test [12] on a 7.2 x 7.2 m continuous slab supported on 16 columns (h = 110 mm) of different sizes (Ø 100 – 320 mm), punching of the four interior columns (C6, C7, C10 and C11) is analysed in this paper;
- Three punching tests with cyclic loading [13] (MRA, MRB and MRC) on 4.2 x 4.2 m slabs with rotationally restrained edges (h = 152 mm);
- Four punching tests [11] (PC1, PC2, PC3 and PC4) with applied sagging moment close to the edges (h = 250 mm).

Table 1 Comparison of the predicted punching strengths to the experimental values (* – cyclic test)

Ref.	Test	$V_{R,test}$ [kN]	$V_{R,test}$ / $V_{R,nomembr.}$	$V_{R,test}$ / $V_{R,membr.}$	Edge conditions
[13]	MRA	458	0.88*	0.80*	$\psi_{mid\text{-}span}$ = as reported (imperfect restraint) $n_{R,mid\text{-}span}$ = 0
	MRB	394	0.87*	0.77*	
	MRC	430	1.00*	0.82*	
[12]	C6	199	1.09	1.03	$\psi_{mid\text{-}span}$ = 0 $n_{R,mid\text{-}span}$ = 0
	C7	332	1.22	1.15	
	C10	303	1.22	1.14	
	C11	454	1.44	1.33	
[11]	PC1	1202	1.17	1.10	$m_{R,r=1420}$ = as reported (applied moment) $n_{R,mid\text{-}span}$ = 0
	PC2	1397	1.24	1.20	
	PC3	1338	1.07	0.98	
	PC4	1431	1.12	1.05	
Mean			1.20	1.12 (only static tests)	
COV			0.10	0.10 (only static tests)	

Table 1 presents the comparison of the results of the analyses to the experimental data. All the tests were analysed firstly by considering only the effect of moment redistribution and neglecting the in-plane forces (applying only the first edge conditions in Table 1) ($V_{R,nomembr.}$) and secondly, also considering the in-plane forces (applying both edge conditions) ($V_{R,membr.}$). Very satisfying correlation between the predictions and the test results is found, considering the complexity of the tests analysed.

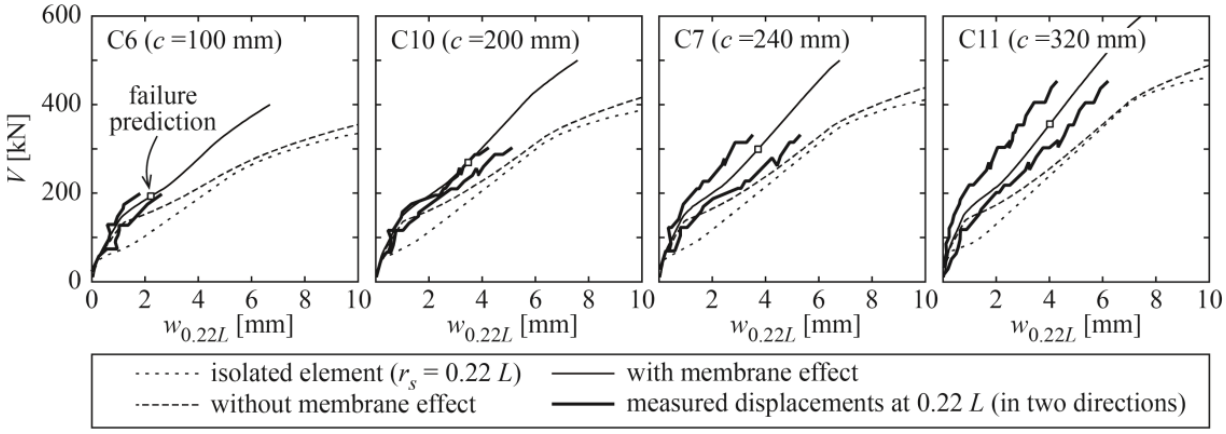

Fig. 6 Measured and predicted load-deformation curves for the interior columns of Ladner's experiment on a continuous slab [12]

Fig. 6 illustrates the application of the model by showing the measured and predicted load-deformation curves for Ladner's experiments [12]. For comparison, the load-rotation curves for the corresponding isolated elements are also shown. It can be observed that the isolated model clearly underestimates the deformations, whereas the continuous model with membrane effect slightly overestimates the stiffness.

6 Conclusions and outlook

This paper presents a numerical model to predict the flexural behaviour and punching shear strength of reinforced concrete flat slabs under distributed loads. Moment redistribution between hogging and sagging moments in continuous slabs as well as the development of in-plane forces due to confinement provided by the external elements and the slab itself are taken into account. Together with the failure criterion of the Critical Shear Crack Theory, the model is able to predict the punching strengths of unconventional punching test specimens with a satisfactory precision.

It is shown that the effects of moment redistribution and membrane forces can greatly increase the punching capacity of flat slabs even without external confining elements.

To become applicable in the design practice, the model should be further validated with comparisons with additional test results and possibly simplified. The influence of the compressive normal forces on the failure criterion should also be further investigated.

References

[1] Ockleston, A. J.: Load tests on a three storey reinforced concrete building in Johannesburg. In: The Structural Engineer 33 (1955) No. 10, pp. 304-322

[2] Ockleston, A. J.: Arching action in reinforced concrete slabs. In: The Structural Engineer 36 (1958) No. 6, pp. 197-201

[3] Wood, R. H.: Plastic and elastic design of slabs and plates, Thames and Hudson (1958)

[4] Braestrup, M. W.: Dome effect in RC slabs: Rigid-plastic analysis. In: Journal of the Structural Division – ASCE (1980) No. 6, pp. 1237-1253

[5] Braestrup, M. W., Morley, C. T.: Dome effect in RC slabs: Elastic-plastic analysis. In: Journal of the Structural Division – ASCE (1980) No. 6, pp. 1255-1262

[6] Amir, S., Walraven, J. C., van der Veen, C.: Compressive membrane action in concrete decks. In: Proceedings of the 9th *fib* international PhD symposium in civil engineering (2012), pp. 91-96

[7] Guandalini, S.: Poinçonnement symétrique des dalles en béton armé. PhD thesis, EPFL No. 3380 (2005), 289 p. (in French)

[8] Guidotti, R.: Poinçonnement des planchers-dalles avec colonnes superposées fortement sollicitées. PhD thesis, EPFL No. 4812 (2010), 230 p. (in French)

[9] Muttoni, A.: Punching shear strength of reinforced concrete slabs without transverse reinforcement. In: ACI Structural Journal (2008) No. 4, pp. 440-450

[10] Fernández Ruiz, M., Muttoni, A.: Applications of Critical Shear Crack Theory to punching of reinforced concrete slabs with transverse reinforcement. In: ACI Structural Journal (2009) No. 4, pp. 485-494

[11] Clément, T.: Influence de la précontrainte sur la résistance au poinçonnement de dalles en béton armé. PhD thesis, EPFL No. 5516 (2012), 222 p. (in French)

[12] Ladner, M., Schaeidt, W., Gut, S.: Experimentelle Untersuchungen an Stahlbeton-Flachdecke. EMPA Bericht Nr. 205 (1977), 96 p. (in German)

[13] Choi, J.-W., Kim, J.-H. J.: Experimental investigations on moment redistribution and punching shear of flat plates. In: ACI Structural Journal (2012) No. 3, pp. 329-338